Brain Imaging and Behavior (2019) 13:493–502
https://doi.org/10.1007/s11682-018-9880-6

ORIGINAL RESEARCH

Altered voxel-wise gray matter structural brain networks in schizophrenia: Association with brain genetic expression pattern

Feng Liu[1] · Hongjun Tian[2] · Jie Li[2] · Shen Li[2] · Chuanjun Zhuo[2]

Published online: 4 May 2018

Abstract

Previous seed- and atlas-based structural covariance/connectivity analyses have demonstrated that patients with schizophrenia is accompanied by aberrant structural connection and abnormal topological organization. However, it remains unclear whether this disruption is present in unbiased whole-brain voxel-wise structural covariance networks (SCNs) and whether brain genetic expression variations are linked with network alterations. In this study, ninety-five patients with schizophrenia and 95 matched healthy controls were recruited and gray matter volumes were extracted from high-resolution structural magnetic resonance imaging scans. Whole-brain voxel-wise gray matter SCNs were constructed at the group level and were further analyzed by using graph theory method. Nonparametric permutation tests were employed for group comparisons. In addition, regression modes along with random effect analysis were utilized to explore the associations between structural network changes and gene expression from the Allen Human Brain Atlas. Compared with healthy controls, the patients with schizophrenia showed significantly increased structural covariance strength (SCS) in the right orbital part of superior frontal gyrus and bilateral middle frontal gyrus, while decreased SCS in the bilateral superior temporal gyrus and precuneus. The altered SCS showed reproducible correlations with the expression profiles of the gene classes involved in therapeutic targets and neurodevelopment. Overall, our findings not only demonstrate that the topological architecture of whole-brain voxel-wise SCNs is impaired in schizophrenia, but also provide evidence for the possible role of therapeutic targets and neurodevelopment-related genes in gray matter structural brain networks in schizophrenia.

Keywords Schizophrenia · Imaging genetic · Gray matter network · Structural covariance strength/density · Gene expression · Graph theory

Introduction

Schizophrenia, characterized by hallucinations, delusions, lack of motivation and impairments of cognitive functions, is a common and severe mental illness with a lifetime prevalence of 1% (Bhugra 2005). Schizophrenia is a disorder related to disruptions of brain connectivity (van den Heuvel and Fornito 2014), and it is also a complex genetic disorder with a heritability of approximately 80% (Lichtenstein et al. 2009).

Recent advances in brain imaging techniques have made it possible to provide a greater understanding of the neuropathology of schizophrenia. Convergent evidence suggests that schizophrenia is linked with abnormalities in brain connectivity (K. Friston 2005; K. J. Friston 1999; van den Heuvel and Fornito 2014). Currently, there are two main approaches for investigating the brain connectivity: functional connectivity derived from functional magnetic resonance imaging (MRI) by calculating correlations between measurements of neuronal activity (i.e., BOLD signal); anatomical connectivity derived from diffusion tensor imaging by tracking white matter fiber pathway between two regions. A growing body of work has reported widespread functional and anatomical dysconnectivity in schizophrenia (van den

Electronic supplementary material The online version of this article (https://doi.org/10.1007/s11682-018-9880-6) contains supplementary material, which is available to authorized users.

✉ Chuanjun Zhuo
chuanjunzhuotjmh@163.com

[1] Department of Radiology and Tianjin Key Laboratory of Functional Imaging, Tianjin Medical University General Hospital, Tianjin 300052, China

[2] Laboratory of Psychiatric Neuroimaging, Tianjin Mental Health Center, Tianjin Anding Hospital, Tianjin Medical University Mental Health Teaching Hospital, No. 13, Liulin Road, Hexi District, Tianjin City 300222, China

Heuvel et al. 2013; Guo et al. 2015). Another prevalent way to investigate the brain connectivity is structural connectivity/covariance derived from high-resolution structural MRI by correlating the inter-regional interdependencies of imaging measurements (e.g., gray matter volume (GMV) or cortical thickness) across subjects. This type of brain connectivity primarily reflects coordination in the development process or the synchronous maturation of different regions of the brain (Evans 2013; Alexander-Bloch et al. 2013), and it has been widely used in researches on Parkinson's disease (Chou et al. 2015), obsessive-compulsive disorder (Subira et al. 2016) and healthy subjects (Zielinski et al. 2010). With regard to schizophrenia, Bassett and colleague's work is the first effort to examine GMV-based structural covariance networks (SCNs) and observe structural disorganization of brain networks in schizophrenia (Bassett et al. 2008). Besides, Zugman et al. have revealed changed node properties of GMV-based SCNs in schizophrenia (Zugman et al. 2015).

However, most of the above-mentioned structural covariance analyses are based on seed-based or atlas-based approaches. Seed-based analysis is a hypothesis-driven approach, which is limited by the requirement for an a priori seed region. The placement of seeds may have considerable influence on the patterns of structural connectivity observed, and there is no way to evaluate which placement is appropriate. Atlas-based analysis is limited by the choice of the parcellation scheme. Previous studies have investigated the impact of template choice on brain networks, and found that different parcellations can lead to significant changes of graph theoretical properties of brain networks (J. Wang et al. 2009; Zalesky et al. 2010). In contrast, whole-brain voxel-based network is not influenced by these factors, and has many desirable characteristics that are not available in region-based networks (Hayasaka and Laurienti 2010). Therefore, in the current study, SCNs were constructed at the whole-brain voxel-level and employed to examine the network property in schizophrenia.

Although recent genome-wide association studies have identified increased number of genes related to the risk of schizophrenia (Ripke et al. 2014; Chen et al. 2015), the neurobiological basis of schizophrenia still remains to be elucidated. The genetic architecture of an imaging phenotype is less complex than that associated with the heterogeneous and more subjective clinical diagnostic criteria of schizophrenia (Guo et al. 2014a, b; Greenwood et al. 2007; Allen et al. 2009). Moreover, investigation of brain imaging phenotypes in the context of transcriptional profiles is a promising avenue for exploring its genetic associations (Romme et al. 2017; Roshchupkin et al. 2016; Ortiz-Teran et al. 2017; Xu et al. 2018). Thus, the aims of the present study were two-fold: we sought to examine whether schizophrenia had voxel-level SCN impairments and, if so, whether these differences were related to the expression patterns of schizophrenia risk genes.

Materials and methods

Subjects

This study was approved by the ethical committee of the Tianjin Medical University General Hospital, and written informed consent was obtained from each subject. The subjects involved were partly from our previous studies (Liu et al. 2016; Zhu et al. 2017). Specifically, ninety-five patients with schizophrenia were recruited and diagnoses were determined by trained psychiatrists using the Structured Clinical Interview for DSM-IV (SCID, patient edition). Among them, six subjects were first-episode patients who had not used medication, and the remaining eighty-nine patients were treated with antipsychotic drug when participating in this study. The Positive and Negative Syndrome Scale (PANSS) was utilized to evaluate the clinical symptoms in patients (Kay et al. 1987). The participant exclusion criteria were 1) poor image quality; 2) left-handedness; 3) younger than 18 years of age or older than 60 years of age; 4) presence of magnetic resonance contraindications; 5) presence of drug abuse or a history of alcohol dependence; 6) presence of intracranial organic lesions and 7) histories of CNS disorders, systemic illnesses, or substance abuse. Ninety-five age-, gender-, handedness-matched healthy controls were recruited from nearby communities and interviewed using the SCID (Non-patient edition) to confirm that none of them had a history of neurological or psychiatric disorder and no gross abnormalities. Additionally, healthy controls had no first-degree relative with any mental disorders.

Data acquisition and preprocessing

The MRI data of all participants were collected using a 3.0 Tesla magnetic resonance scanner (Discovery MR750, General Electric, Milwaukee, WI, USA) at the Tianjin Medical University General Hospital. Foam paddings were utilized to minimize head movement and earplugs were employed to reduce scanner noise. During data acquisition, the participants were asked to hold still and move as little as possible. Sagittal 3D high-resolution T1WI structural images were acquired by a brain volume scanning sequence with scanning parameters as follows: repetition time = 8.2 ms; echo time = 3.2 ms; inversion time = 450 ms; flip angle = 12°; field of view = 256 mm × 256 mm; matrix = 256 × 256; slice thickness = 1 mm, no gap; and 188 slices.

GMVs were extracted by using the standard pipeline of the CAT12 toolbox (version r1278, http://dbm.neuro.uni-jena.de/cat), which is an extension to SPM12 software (http://www.fil.ion.ucl.ac.uk/spm). All T1-weighted images were first corrected for bias-field inhomogeneities, and then the corrected images were affine registered to standard space and segmented into grey matter, white matter, and cerebrospinal fluid. Next, the segmented images were spatially normalized using the

DARTEL algorithm (Ashburner 2007). To preserve the absolute volume of gray matter, modulation was performed on the normalized grey matter images by multiplying the voxel values with the Jacobian determinant (both linear and non-linear components) derived from the spatial normalization.

Voxel-based gray matter covariance network analysis

For computational efficiency, the gray matter images were down-sampled to 3-mm isotropic voxels. A linear regression was subsequently performed at each voxel to remove the effects of age, gender and intracranial brain volume. The residuals of this regression were then substituted for the raw gray matter values for the following analysis.

For each group, the gray matter covariance between two voxels was measured by computing the Pearson correlation coefficient across subjects. The structural covariance/connectivity strength (SCS) for each voxel was calculated by the weighted sum of survived correlations of other voxels, and the SCS map of each group could be obtained. A threshold of $r > 0.2$ for the correlation coefficient to remove weak correlations possibly arising from noise signals. Such an SCS metric is also known as the "degree centrality" of weighted networks in terms of the graph theory (Buckner et al. 2009; Liu et al. 2015b). The original SCS value of each voxel was divided by the global mean SCS value for standardization purpose, and the mean SCS maps were subsequently spatially smoothed with an 8-mm full width at half-maximum Gaussian kernel (Liu et al. 2013). Notably, SCS computation was constrained within a cortical gray matter mask (32,164 voxels), which was created by the following procedures: 1) all the normalized gray matter density images from healthy subjects were averaged and a threshold of 0.2 was used to create a study-specific gray matter mask; 2) the subcortical regions and cerebellar areas in the Anatomical Automatic Labeling (AAL) atlas were removed and a cortical AAL mask was acquired; 3) these two masks were intersected and the final cortical gray matter mask was obtained.

Statistical analysis

Since only group-level results were obtained from the covariance network analysis, permutation test was employed to examine SCS differences (Liu et al. 2015a; Liu et al. 2017). Briefly, the between-group real difference of the two SCS maps was initially computed (subtracting control group's mean SCS image from schizophrenia group's mean SCS image). All subjects' gray matter images were then randomly reallocated to each group by keeping the number of subjects in each group unchanged, and repeated network construction, SCS calculation and between-group subtraction. For each voxel, we counted the number of times that randomized difference in permutations was higher than real difference (two-tailed). After dividing by the total number of permutations (1000 permutations), the uncorrected p value was acquired for each voxel. Notably, linear regression analysis was conducted before the permutation test to remove the confounding effects of age, gender and intracranial brain volume. Finally, a Benjamini–Hochberg false discovery rate (BH-FDR) correction ($q < 0.05$) was employed to find the significant SCS difference.

Gene expression

Publicly available gene expression data were obtained from Allen Human Brain Atlas (AHBA) that provides comprehensive coverage of the normal adult brain (Hawrylycz et al. 2012). In the current study, the AHBA dataset was used to extract gene expression profiles, which consists of normalized microarray expression data of 20,737 genes represented by 58,692 probes (measured in 3702 brain samples from six human postmortem neurotypical adult brains). Based on the current hypotheses of schizophrenia aetiology or treatment strategies, the schizophrenia working group of the Psychiatric Genomics Consortium divided 36 schizophrenia risk genes (Supplementary Table S1) into six specific classes (Ripke et al. 2014): 1) therapeutic targets (two genes); 2) glutamatergic neurotransmission (six genes); 3) neuronal calcium signaling (seven genes); 4) synaptic function and plasticity (nine genes); 5) other neuronal ion channels (five genes); 6) neurodevelopment (seven genes).

To determine whether expression of gene in these classes was correlated with between-group SCS difference, the following procedures were performed: 1) the average gene expression were calculated for each class. Of note, if there were multiple probes sampling the same gene, expression values from all these probes were averaged for each gene; 2) seed regions were defined as 6-mm radius spheres (2 times of the voxel size) centered on each sample within cortical gray matter mask, and the mean between-group SCS changes in these seeds were extracted; 3) regression models with random effect analyses (calculated correlations in each of six donors, and then evaluated the significance using one-sample t-tests) were utilized to examine the correlation between SCS difference and gene expression of each class across all the above-mentioned samples. Furthermore, we carried out an exploratory analysis by investigating the relationship between each gene in the AHBA database (20,737 genes) and SCS difference using the same regression models to identify new candidate schizophrenia risk genes. All these results were corrected using BH-FDR correction ($q < 0.05$).

Validation analysis

We conducted three analyses to evaluate the reproducibility of our findings. First, a correlation coefficient threshold of 0.2 was utilized in the SCS computation to remove weak

correlations possibly arising from signal noise. We recalculated SCS using two other different correlation thresholds (0.1 and 0.3) to investigate whether our main results relied on the choices of thresholds. Second, since weighted edges can more accurately characterize the brain network, the weighted SCNs were constructed in the present study. However, compared with the binarized networks, the weighted ones may be more sensitive to noise. Therefore, we constructed the binarized SCNs and calculated SCS (also known as structural covariance density (SCD)) to test the effect of network types on our results. Finally, the raw gray matter images were resampled to 3-mm isotropic voxels due to highly computational burden. Here, the raw resolution (1.5-mm isotropic voxels, a total of 258,610 voxels, 3-mm radius sphere centered on each sample in the gene expression analyses) along with the correlation coefficient threshold of 0.2 was adopted and weighted SCNs were constructed to explore the influence of the image resolution on our findings.

Results

Demographics and clinical characteristics of the participants

The demographic and clinical data are shown in Table 1. Gender (50 males for the schizophrenia group and 47 males for the control group; $p = 0.663$), age (34.25 ± 8.34 years for the schizophrenia group; 34.27 ± 10.88 years for the control group; $p = 0.988$) and handedness (all the participants in two groups are right-handed) were matched between the two groups. In addition, the illness duration, the PANSS positive score, negative score and general score in the schizophrenia group were 119.93 ± 92.28 months, 16.73 ± 7.91, 19.96 ± 9.05 and 33.82 ± 11.00, respectively.

Table 1 Demographics and clinical characteristics of the participants

Variables (Mean ± SD)	Schizophrenia	HC	*P* value
Gender (male/female)	50/45	47/48	0.663[a]
Age (years)	34.25 ± 8.34	34.27 ± 10.88	0.988[b]
Handedness (right/left)	95/0	95/0	–
Duration (months)	119.93 ± 92.28	–	–
PANSS			
Positive score	16.73 ± 7.91	–	–
Negative score	19.96 ± 9.05	–	–
General score	33.82 ± 11.00	–	–

[a] *p*-value was obtained by a chi-square test; [b] *p*-value was obtained by a two-sample *t*-test. Abbreviations: SD, standard deviation; HC, healthy control; PANSS, positive and negative syndrome scale

Within-group and between-group SCS analyses

The within-group SCS maps are shown in Fig. 1a. The spatial distributions of brain areas with high SCS were similar across the two groups despite some differences in strength. Those highly connected areas (i.e., higher SCS) were mainly distributed in medial prefrontal cortex, posterior cingulate cortex/precuneus, insula and lateral prefrontal and temporal regions. The between-group subtraction map together with raw *p* map is shown in Supplementary Fig. S1A. After BH-FDR correction, patients with schizophrenia exhibited significantly increased SCS in the right orbital part of superior frontal gyrus, bilateral middle frontal gyrus, while significantly decreased SCS in the bilateral superior temporal gyrus and precuneus (Fig. 2).

Gene expression

The relationships between the SCS alterations and the pattern of gene expression were examined. All gene classes could not survive BH-FDR correction (see the first column in Table 2). The class of genes involved in therapeutic targets ($p_{adj} = 0.0512$), neuronal calcium signaling ($p_{adj} = 0.0696$), other neuronal ion channels ($p_{adj} = 0.0512$) and neurodevelopment ($p_{adj} = 0.0512$) showed trends for associations. Furthermore, 355 genes were identified by examining the correlations between all AHBA genes and SCS alterations (see the first column in Supplementary Table S2).

Validations

As presented in Figs. 1, S1 and 3, Tables 2 and S2, we found that our main results (weighted network, $r = 0.2$, voxel size = $3 \times 3 \times 3$ mm^3) were largely reproducible in validation analyses of the binarized network ($r = 0.2$, voxel size = $3 \times 3 \times 3$ mm^3), the weighted network with different correlation thresholds ($r = 0.1$ and 0.3, voxel size = $3 \times 3 \times 3$ mm^3) and the weighted network with raw image resolution ($r = 0.2$, voxel size = $1.5 \times 1.5 \times 1.5$ mm^3). Particularly, in the gene expression analyses, two gene classes (therapeutic targets and neurodevelopment) had all $ps < 0.05$ (uncorrected) across a range of analytical choices (see Table 2 for details), indicating reliably correlations of these class of genes on SCS alterations in schizophrenia. In addition, 49 genes survived BH-FDR correction in all the five aforementioned methods (Supplementary Table 2).

Discussion

To our knowledge, this study represents the first attempt to investigate the whole-brain voxel-wise SCNs disturbance in schizophrenia. By means of graph theory, we found that

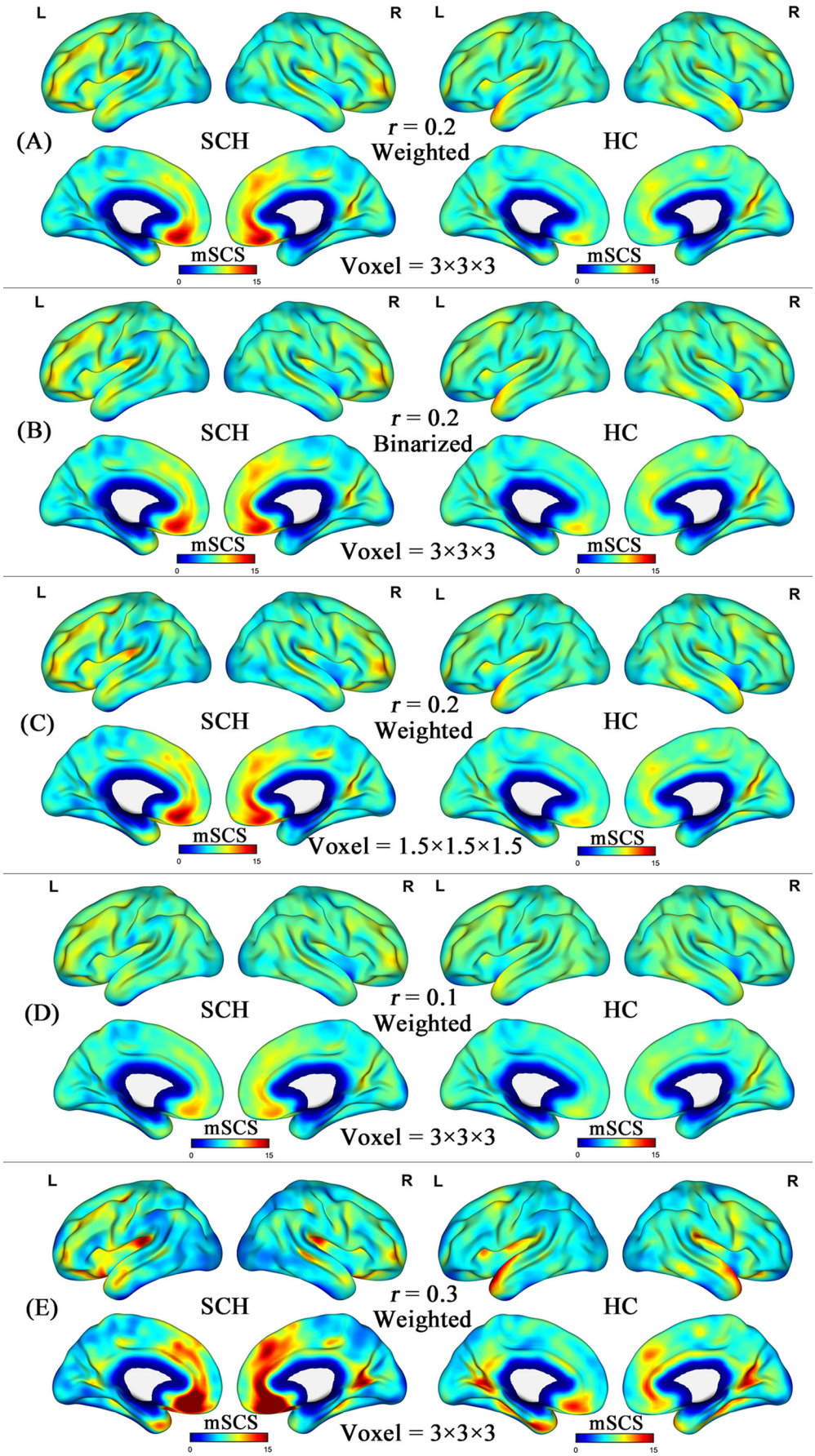

Fig. 1 Within-group structural covariance strength (SCS) maps for schizophrenia group (left panel) and healthy control group (right panel) across a range of analytical approaches: (**a**) weighted network, correlation threshold = 0.2, voxel size = 3 × 3 × 3 mm^3; (**b**) binarized network, correlation threshold = 0.2, voxel size = 3 × 3 × 3 mm^3; (**c**) weighted network, correlation threshold = 0.2, voxel size = 1.5 × 1.5 × 1.5 mm^3; (**d**) weighted network, correlation threshold = 0.1, voxel size = 3 × 3 × 3 mm^3; (**e**) weighted network, correlation threshold = 0.3, voxel size = 3 × 3 × 3 mm^3. The SCS maps were visualized with the BrainNet Viewer (Xia et al. 2013). Abbreviation: SCH, schizophrenia; HC, healthy controls; mSCS, mean structural covariance strength; L, left; R, right

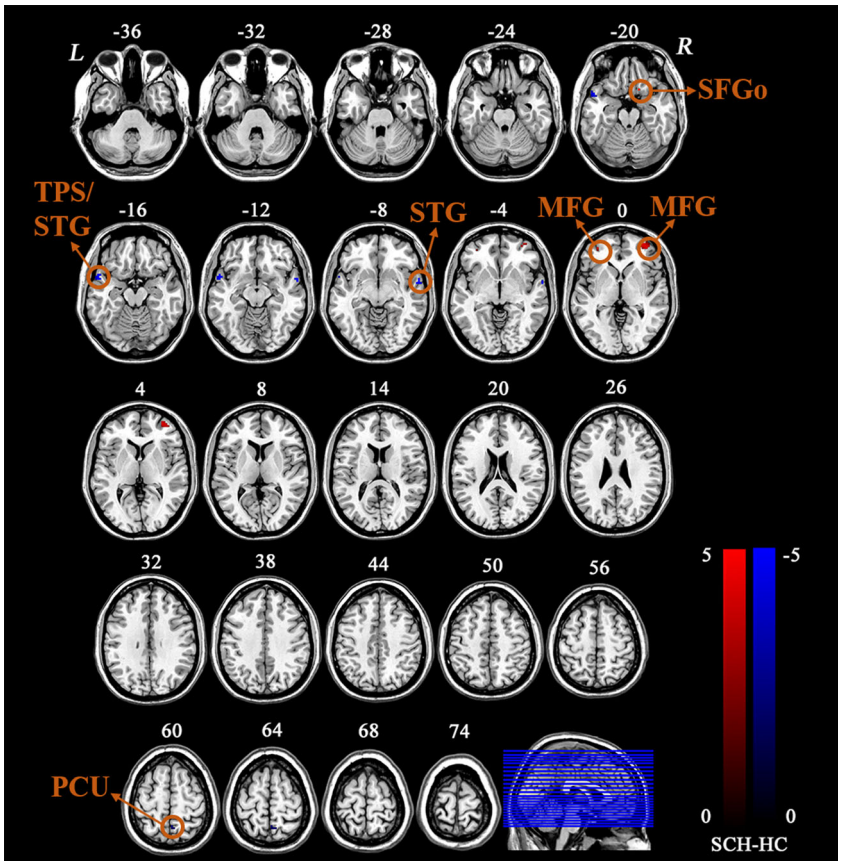

Fig. 2 Significant structural covariance strength (SCS) differences revealed by permutation test between patients with schizophrenia and healthy controls. The threshold was set at $q < 0.05$ with Benjamini–Hochberg false discovery rate correction. The network constructed parameters were: weighted network, correlation threshold = 0.2 and voxel size = 3 × 3 × 3 mm^3. The colorbar represents the magnitude of mean SCS difference. Abbreviation: SCH, schizophrenia; HC, healthy controls; SFGo, orbital part of superior frontal gyrus; MFG, middle frontal gyrus; STG, superior temporal gyrus; TPS, superior part of temporal pole; PCU, precuneus; L, left; R, right

Table 2 Relationships between gene expression of each gene classes and SCS changes across five analytical methods

	Method 1 (t / p value)	Method 2 (t / p value)	Method 3 (t / p value)	Method 4 (t / p value)	Method 5 (t / p value)
Class 1	$t = 3.1430$ $p_{raw} = 0.0256$ $p_{adj} = 0.0512$	$t = 3.1413$ $p_{raw} = 0.0256$ $p_{adj} = 0.0541$	$t = 2.6557$ $p_{raw} = 0.0451$ $p_{adj} = 0.1467$	$t = 3.1224$ $p_{raw} = 0.0262$ $p_{adj} = 0.0699$	$t = 3.1593$ $p_{raw} = 0.0251$ $p_{adj} = 0.0406$
Class 2	$t = 1.8138$ $p_{raw} = 0.1294$ $p_{adj} = 0.1553$	$t = 1.9030$ $p_{raw} = 0.1154$ $p_{adj} = 0.1385$	$t = 1.6590$ $p_{raw} = 0.1580$ $p_{adj} = 0.1896$	$t = 2.0566$ $p_{raw} = 0.0948$ $p_{adj} = 0.1138$	$t = 1.1436$ $p_{raw} = 0.3046$ $p_{adj} = 0.3655$
Class 3	$t = 2.6322$ $p_{raw} = 0.0464$ $p_{adj} = 0.0696$	$t = 2.5862$ $p_{raw} = 0.0491$ $p_{adj} = 0.0736$	$t = 1.6975$ $p_{raw} = 0.1504$ $p_{adj} = 0.1896$	$t = 2.5103$ $p_{raw} = 0.0538$ $p_{adj} = 0.0807$	$t = -3.0924$ $p_{raw} = 0.0271$ $p_{adj} = 0.0406$
Class 4	$t = -0.0910$ $p_{raw} = 0.9310$ $p_{adj} = 0.9310$	$t = -0.0327$ $p_{raw} = 0.9752$ $p_{adj} = 0.9752$	$t = -0.3848$ $p_{raw} = 0.7162$ $p_{adj} = 0.7162$	$t = 0.0502$ $p_{raw} = 0.9619$ $p_{adj} = 0.9619$	$t = -0.5163$ $p_{raw} = 0.6277$ $p_{adj} = 0.6277$
Class 5	$t = -3.1449$ $p_{raw} = 0.0255$ $p_{adj} = 0.0512$	$t = -3.0939$ $p_{raw} = 0.0270$ $p_{adj} = 0.0541$	$t = -1.7008$ $p_{raw} = 0.1497$ $p_{adj} = 0.1896$	$t = -2.8705$ $p_{raw} = 0.0350$ $p_{adj} = 0.0699$	$t = -3.4483$ $p_{raw} = 0.0183$ $p_{adj} = 0.0406$
Class 6	$t = 3.4272$ $p_{raw} = 0.0187$ $p_{adj} = 0.0512$	$t = 3.4180$ $p_{raw} = 0.0189$ $p_{adj} = 0.0541$	$t = 2.5891$ $p_{raw} = 0.0489$ $p_{adj} = 0.1467$	$t = 3.4121$ $p_{raw} = 0.0190$ $p_{adj} = 0.0699$	$t = 3.3822$ $p_{raw} = 0.0196$ $p_{adj} = 0.0406$

t values are obtained by regression models with random effect analyses. p_{raw} is raw p value corresponding to t value and p_{adj} is BH-FDR adjusted p value. Analytical method 1: weighted network, correlation threshold = 0.2, voxel size = 3 × 3 × 3 mm^3; method 2: binarized network, correlation threshold = 0.2, voxel size = 3 × 3 × 3 mm^3; method 3: weighted network, correlation threshold = 0.2, voxel size = 1.5 × 1.5 × 1.5 mm^3; method 4: weighted network, correlation threshold = 0.1, voxel size = 3 × 3 × 3 mm^3; method 5: weighted network, correlation threshold = 0.3, voxel size = 3 × 3 × 3 mm^3. Gene class 1: therapeutic targets; class 2: glutamatergic neurotransmission; class 3: neuronal calcium signaling; class 4: synaptic function and plasticity; class 5: other neuronal ion channels; class 6: neurodevelopment

patients exhibited higher SCS values in the right orbital part of superior frontal gyrus and bilateral middle frontal gyrus but lower SCS in the bilateral superior temporal gyrus and precuneus than healthy controls. Moreover, the expressions of schizophrenia risk genes associated with therapeutic targets and neurodevelopment were found to be coincided with SCS alterations. These results shed new light on the pathophysiological mechanisms underlying schizophrenia and suggest the feasibility of using gene expression to investigate this disorder.

The degree centrality was selected as the network attribute to investigate schizophrenia in the present study rather than other centrality measures. The rationale behind this choice can be generally characterized as three folds: first, node degree is a simple, direct and one of the most important network centrality measures; second, it is the most reliable and resilient metric of centrality measures in brain network (J. H. Wang et al. 2011); and finally, it is difficult to calculate other nodal metrics (e.g., betweenness or efficiency) in a such huge voxel-based network with tens of thousands of nodes. From the within-group SCS maps, we found that structural hubs (i.e., higher SCS) were predominantly located in the default-mode regions (medial prefrontal cortex and posterior cingulate cortex/precuneus), insula, and lateral prefrontal and temporal regions (Fig. 1), exhibiting a large overlap with the hubs acquired from resting-state functional MRI and anatomical hubs obtained from diffusion tensor imaging. Although both groups showed similar hub distributions, significant SCS alterations were observed from between-group comparisons: stronger SCS in the right orbital part of superior frontal gyrus, bilateral middle frontal gyrus and weaker SCS in the bilateral superior temporal gyrus and precuneus were found in schizophrenia. Although previous neuroimaging literature has documented GMV changes in these areas (Honea et al. 2008; Guo et al. 2014a, b; Kikinis et al. 2010), we first revealed the alterations in these regions from a voxel-wise whole-brain network perspective. As shown in Fig. 3, we overlapped significant between-group SCS results and the middle frontal gyrus was consistently observed across all five analytical methods, indicating a reproducible finding of this region. Given that accumulating evidence from voxel-based morphometry studies reported GMV reduction in middle frontal gyrus (Tregellas et al. 2007; Kikinis et al. 2010; Anderson et al. 2015), increased structural connections potentially indicated a compensatory mechanism for regional abnormalities.

The SCS abnormalities in schizophrenia were found to be correlated with the expression of therapeutic targets and neurodevelopment-related genes. The genes in therapeutic targets class include *DRD2* and *GRM3*. Specifically, the *DRD2* gene encodes dopamine receptor D2, which is of particular interest in psychiatry and the main receptor for the majority

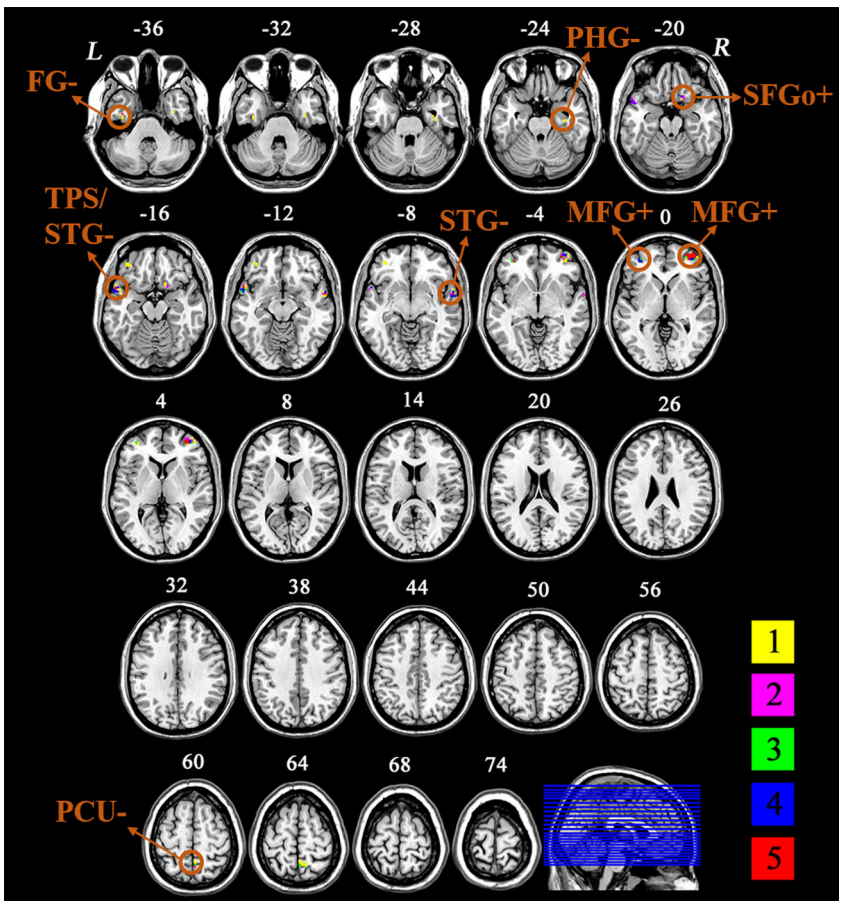

Fig. 3 Overlap of significant between-group structural covariance strength (SCS) results. For each voxel, the color represents the number of tests where this voxel showed significant group differences across the five analytical approaches. As shown in bottom right corner, red, blue, green, violet and yellow color denote the overlap times" of five, four, three, two and one, respectively. Additionally, the signs "+" and "-" in the figure indicate significantly higher and lower SCS of this region in schizophrenia, respectively. Abbreviation: SFGo, orbital part of superior frontal gyrus; MFG, middle frontal gyrus; STG, superior temporal gyrus; TPS, superior part of temporal pole; PCU, precuneus; PHG, parahippocampal gyrus; FG, fusiform gyrus; L, left; R, right

of antipsychotic drugs; the *GRM3* gene encodes metabotropic glutamate receptor 3 that has been extensively investigated as a possible therapeutic target in schizophrenia (Ripke et al. 2014). In addition, multiple lines of evidence suggest that schizophrenia is a neurodevelopment disorder (Insel 2010; Fatemi and Folsom 2009). Genes associated with cell migration and proliferation, myelination, axonal outgrowth, synaptogenesis and apoptosis are abnormal in schizophrenia, indicating a neurodevelopmental etiology of schizophrenia (Fatemi and Folsom 2009). The expressions of these schizophrenia risk gene classes are correlated to the SCS changes, shedding light on the potential genetic associations of SCNs disruptions in the disorder. Furthermore, we found that 355 genes in AHBA database had a close relationship with anomalous SCS; and among them, 49 genes passed the BH-FDR correction in all validations (Supplementary Table S2), which may serve as new candidate schizophrenia risk genes. Some of these genes (e.g., *AUTS2* (Zhang et al. 2014), *AGA* (Rowland et al. 2017), and *HDAC9* (Tam et al. 2010)) have indeed been demonstrated to be implicated in schizophrenia. Together, combining gene expression and image phenotype could be a valuable tool for better understanding the structural network changes in schizophrenia.

Several limitations of this study merit consideration. First, most of the patients were chronic schizophrenia with mixed symptoms and medicated. Therefore, our results might be confounded by the use of antipsychotics. Moreover, the duration of treatment is different for the patients, which may also affect the results of this study. However, only six patients were first-episode who had not used medication. The group-level network construction manner cannot be reliable based on such small sample size (six cases). In the future, first-episode, drug-naive patients with a large sample size will be recruited to confirm our findings and clarify the effect of drugs on SCS. Second, we cannot examine relationships between the altered SCS and clinical characteristics due to the group level network. Finally, the used gene expression data are non-East Asian gene expression profiles from the AHBA. Currently, there is no East Asian gene expression dataset and AHBA is the only source of high-resolution gene expression data. Future studies using an Asian brain gene expression profiles should perform to replicate the findings of our study.

Conclusions

Here, we examined whole-brain voxel-wise GMV-based SCNs in schizophrenia. We found that, although both patients and healthy control groups had similar SCS patterns, the patients had significantly changed SCS in several brain areas. In addition, the altered SCS was observed to be correlated with expression of genes associated with therapeutic targets and neurodevelopment. These results had proven to be robust after considering the effects of different analytical methods. In summary, we demonstrated a disruption of voxel-wise SCNs and extended the current understanding of the neuropathological underpinnings of schizophrenia.

Funding This study was funded by grants from the National Natural Science Foundation of China (81501451 to F.L.), the Natural Science Foundation of Tianjin (16JCYBJC24200 to J.L. and 17JCZDJC35700 to C.Z.), the Tianjin Health Bureau Foundation (2014KR02 to C.Z.), the Tianjin Health Key Program (13KG118 to J.L.), and the "New Century" Talent Training Project of Tianjin Medical University General Hospital (2017 to F.L.)

Compliance with ethical standards

Conflict of interest All the authors declare that they have no conflict of interest.

Ethical approval This study was approved by the ethical committee of the Tianjin Medical University General Hospital.

Informed consent Written informed consent was obtained from all participants.

References

Allen, A. J., Griss, M. E., Folley, B. S., Hawkins, K. A., & Pearlson, G. D. (2009). Endophenotypes in schizophrenia: A selective review. *Schizophrenia Research, 109*(1–3), 24–37.

Anderson, V. M., Goldstein, M. E., Kydd, R. R., & Russell, B. R. (2015). Extensive gray matter volume reduction in treatment-resistant schizophrenia. *The International Journal of Neuropsychopharmacology, 18*(7), pyv016.

Ashburner, J. (2007). A fast diffeomorphic image registration algorithm. *NeuroImage, 38*(1), 95–113.

Alexander-Bloch, A., Giedd, J. N., & Bullmore, E. (2013). Imaging structural co-variance between human brain regions. *Nature Reviews Neuroscience, 14*(5), 322–336.

Bassett, D. S., Bullmore, E., Verchinski, B. A., Mattay, V. S., Weinberger, D. R., & Meyer-Lindenberg, A. (2008). Hierarchical organization of human cortical networks in health and schizophrenia. *The Journal of Neuroscience, 28*(37), 9239–9248.

Bhugra, D. (2005). The global prevalence of schizophrenia. PLoS Medicine, 2(5), e151.

Buckner, R. L., Sepulcre, J., Talukdar, T., Krienen, F. M., Liu, H., Hedden, T., Andrews-Hanna, J. R., Sperling, R. A., & Johnson, K. A. (2009). Cortical hubs revealed by intrinsic functional connectivity: Mapping, assessment of stability, and relation to Alzheimer's disease. *The Journal of Neuroscience, 29*(6), 1860–1873.

Chen, J., Cao, F., Liu, L., Wang, L., & Chen, X. (2015). Genetic studies of schizophrenia: An update. *Neuroscience Bulletin, 31*(1), 87–98.

Chou, K. H., Lin, W. C., Lee, P. L., Tsai, N. W., Huang, Y. C., Chen, H. L., Cheng, K. Y., Chen, P. C., Wang, H. C., Lin, T. K., Li, S. H., Lin, W. M., Lu, C. H., & Lin, C. P. (2015). Structural covariance networks of striatum subdivision in patients with Parkinson's disease. *Human Brain Mapping, 36*(4), 1567–1584.

Evans, A. C. (2013). Networks of anatomical covariance. *NeuroImage, 80*, 489–504.

Fatemi, S. H., & Folsom, T. D. (2009). The neurodevelopmental hypothesis of schizophrenia, revisited. *Schizophrenia Bulletin, 35*(3), 528–548.

Friston, K. J. (1999). Schizophrenia and the disconnection hypothesis. *Acta Psychiatrica Scandinavica Supplementum, 395*, 68–79.

Friston, K. (2005). Disconnection and cognitive dysmetria in schizophrenia. *The American Journal of Psychiatry, 162*(3), 429–432.

Greenwood, T. A., Braff, D. L., Light, G. A., Cadenhead, K. S., Calkins, M. E., Dobie, D. J., Freedman, R., Green, M. F., Gur, R. E., Gur, R. C., Mintz, J., Nuechterlein, K. H., Olincy, A., Radant, A. D., Seidman, L. J., Siever, L. J., Silverman, J. M., Stone, W. S., Swerdlow, N. R., Tsuang, D. W., Tsuang, M. T., Turetsky, B. I., & Schork, N. J. (2007). Initial heritability analyses of endophenotypic measures for schizophrenia: The consortium on the genetics of schizophrenia. *Archives of General Psychiatry, 64*(11), 1242–1250.

Guo, W., Hu, M., Fan, X., Liu, F., Wu, R., Chen, J., et al. (2014a). Decreased gray matter volume in the left middle temporal gyrus as a candidate biomarker for schizophrenia: A study of drug naive, first-episode schizophrenia patients and unaffected siblings. *Schizophrenia Research, 159*(1), 43–50.

Guo, X., Li, J., Wang, J., Fan, X., Hu, M., Shen, Y., et al. (2014b). Hippocampal and orbital inferior frontal gray matter volume abnormalities and cognitive deficit in treatment-naive, first-episode patients with schizophrenia. Schizophrenia Research, 152(2–3), 339–343.

Guo, W., Liu, F., Xiao, C., Liu, J., Yu, M., Zhang, Z., et al. (2015). Increased short-range and long-range functional connectivity in first-episode, medication-naive schizophrenia at rest. Schizophrenia Research, 166(1–3), 144–150.

Hawrylycz, M. J., Lein, E. S., Guillozet-Bongaarts, A. L., Shen, E. H., Ng, L., Miller, J. A., van de Lagemaat, L. N., Smith, K. A., Ebbert, A., Riley, Z. L., Abajian, C., Beckmann, C. F., Bernard, A., Bertagnolli, D., Boe, A. F., Cartagena, P. M., Chakravarty, M. M., Chapin, M., Chong, J., Dalley, R. A., Daly, B. D., Dang, C., Datta, S., Dee, N., Dolbeare, T. A., Faber, V., Feng, D., Fowler, D. R., Goldy, J., Gregor, B. W., Haradon, Z., Haynor, D. R., Hohmann, J. G., Horvath, S., Howard, R. E., Jeromin, A., Jochim, J. M., Kinnunen, M., Lau, C., Lazarz, E. T., Lee, C., Lemon, T. A., Li, L., Li, Y., Morris, J. A., Overly, C. C., Parker, P. D., Parry, S. E., Reding, M., Royall, J. J., Schulkin, J., Sequeira, P. A., Slaughterbeck, C. R., Smith, S. C., Sodt, A. J., Sunkin, S. M., Swanson, B. E., Vawter, M. P., Williams, D., Wohnoutka, P., Zielke, H. R., Geschwind, D. H., Hof, P. R., Smith, S. M., Koch, C., Grant, S. G. N., & Jones, A. R. (2012). An anatomically comprehensive atlas of the adult human brain transcriptome. *Nature, 489*(7416), 391–399.

Hayasaka, S., & Laurienti, P. J. (2010). Comparison of characteristics between region-and voxel-based network analyses in resting-state fMRI data. *NeuroImage, 50*(2), 499–508.

Honea, R. A., Meyer-Lindenberg, A., Hobbs, K. B., Pezawas, L., Mattay, V. S., Egan, M. F., Verchinski, B., Passingham, R. E., Weinberger, D. R., & Callicott, J. H. (2008). Is gray matter volume an intermediate phenotype for schizophrenia? A voxel-based morphometry study of patients with schizophrenia and their healthy siblings. *Biological Psychiatry, 63*(5), 465–474.

Insel, T. R. (2010). Rethinking schizophrenia. *Nature, 468*(7321), 187–193.

Kay, S. R., Fiszbein, A., & Opler, L. A. (1987). The positive and negative syndrome scale (PANSS) for schizophrenia. *Schizophrenia Bulletin, 13*(2), 261–276.

Kikinis, Z., Fallon, J. H., Niznikiewicz, M., Nestor, P., Davidson, C., Bobrow, L., Pelavin, P. E., Fischl, B., Yendiki, A., McCarley, R. W., Kikinis, R., Kubicki, M., & Shenton, M. E. (2010). Gray matter volume reduction in rostral middle frontal gyrus in patients with chronic schizophrenia. *Schizophrenia Research, 123*(2–3), 153–159.

Lichtenstein, P., Yip, B. H., Bjork, C., Pawitan, Y., Cannon, T. D., Sullivan, P. F., et al. (2009). Common genetic determinants of schizophrenia and bipolar disorder in Swedish families: A population-based study. *Lancet, 373*(9659), 234–239.

Liu, F., Guo, W., Liu, L., Long, Z., Ma, C., Xue, Z., Wang, Y., Li, J., Hu, M., Zhang, J., du, H., Zeng, L., Liu, Z., Wooderson, S. C., Tan, C., Zhao, J., & Chen, H. (2013). Abnormal amplitude low-frequency oscillations in medication-naive, first-episode patients with major depressive disorder: A resting-state fMRI study. *Journal of Affective Disorders, 146*(3), 401–406.

Liu, F., Guo, W., Fouche, J. P., Wang, Y., Wang, W., Ding, J., Zeng, L., Qiu, C., Gong, Q., Zhang, W., & Chen, H. (2015a). Multivariate classification of social anxiety disorder using whole brain functional connectivity. *Brain Structure & Function, 220*(1), 101–115.

Liu, F., Zhu, C., Wang, Y., Guo, W., Li, M., Wang, W., Long, Z., Meng, Y., Cui, Q., Zeng, L., Gong, Q., Zhang, W., & Chen, H. (2015b). Disrupted cortical hubs in functional brain networks in social anxiety disorder. *Clinical Neurophysiology, 126*(9), 1711–1716.

Liu, F., Zhuo, C., & Yu, C. (2016). Altered cerebral blood flow covariance network in schizophrenia. *Frontiers in Neuroscience, 10*, 308.

Liu, F., Wang, Y., Li, M., Wang, W., Li, R., Zhang, Z., Lu, G., & Chen, H. (2017). Dynamic functional network connectivity in idiopathic generalized epilepsy with generalized tonic-clonic seizure. *Human Brain Mapping, 38*(2), 957–973.

van den Heuvel, M. P., & Fornito, A. (2014). Brain networks in schizophrenia. *Neuropsychology Review, 24*(1), 32–48.

van den Heuvel, M. P., Sporns, O., Collin, G., Scheewe, T., Mandl, R. C., Cahn, W., et al. (2013). Abnormal rich club organization and functional brain dynamics in schizophrenia. *JAMA Psychiatry, 70*(8), 783–792.

Ortiz-Teran, L., Diez, I., Ortiz, T., Perez, D. L., Aragon, J. I., Costumero, V., et al. (2017). Brain circuit-gene expression relationships and neuroplasticity of multisensory cortices in blind children. *Proceedings of the National Academy of Sciences of the United States of America, 114*(26), 6830–6835.

Ripke, S., Neale, B. M., Corvin, A., Walters, J. T., Farh, K.-H., Holmans, P. A., et al. (2014). Biological insights from 108 schizophrenia-associated genetic loci. *Nature, 511*(7510), 421.

Romme, I. A., de Reus, M. A., Ophoff, R. A., Kahn, R. S., & van den Heuvel, M. P. (2017). Connectome Disconnectivity and cortical gene expression in patients with schizophrenia. *Biological Psychiatry, 81*(6), 495–502.

Roshchupkin, G. V., Adams, H. H., van der Lee, S. J., Vernooij, M. W., van Duijn, C. M., Uitterlinden, A. G., van der Lugt, A., Hofman, A., Niessen, W. J., & Ikram, M. A. (2016). Fine-mapping the effects of Alzheimer's disease risk loci on brain morphology. *Neurobiology of Aging, 48*, 204–211.

Rowland, L. M., Demyanovich, H. K., Wijtenburg, S. A., Eaton, W. W., Rodriguez, K., Gaston, F., Cihakova, D., Talor, M. V., Liu, F., McMahon, R. R., Hong, L. E., & Kelly, D. L. (2017). Antigliadin antibodies (AGA IgG) are related to neurochemistry in schizophrenia. *Frontiers in Psychiatry, 8*, 104.

Subira, M., Cano, M., de Wit, S. J., Alonso, P., Cardoner, N., Hoexter, M. Q., et al. (2016). Structural covariance of neostriatal and limbic regions in patients with obsessive-compulsive disorder. *Journal of Psychiatry & Neuroscience, 41*(2), 115–123.

Tam, G. W., van de Lagemaat, L. N., Redon, R., Strathdee, K. E., Croning, M. D., Malloy, M. P., et al. (2010). Confirmed rare copy number variants implicate novel genes in schizophrenia. *Biochemical Society Transactions, 38*(2), 445–451.

Tregellas, J. R., Shatti, S., Tanabe, J. L., Martin, L. F., Gibson, L., Wylie, K., & Rojas, D. C. (2007). Gray matter volume differences and the effects of smoking on gray matter in schizophrenia. *Schizophrenia Research, 97*(1–3), 242–249.

Wang, J., Wang, L., Zang, Y., Yang, H., Tang, H., Gong, Q., Chen, Z., Zhu, C., & He, Y. (2009). Parcellation-dependent small-world brain functional networks: A resting-state fMRI study. *Human Brain Mapping, 30*(5), 1511–1523.

Wang, J. H., Zuo, X. N., Gohel, S., Milham, M. P., Biswal, B. B., & He, Y. (2011). Graph theoretical analysis of functional brain networks:

Test-retest evaluation on short- and long-term resting-state functional MRI data. *PLoS One, 6*(7), e21976.

Xia, M., Wang, J., & He, Y. (2013). BrainNet viewer: A network visualization tool for human brain connectomics. *PLoS One, 8*(7), e68910.

Xu, Q., Fu, J., Liu, F., Qin, W., Liu, B., Jiang, T., et al. (2018). Left parietal functional connectivity mediates the association between COMT rs4633 and verbal intelligence in healthy adults. *Frontiers in Neuroscience, 12*(233). https://doi.org/10.3389/fnins.2018.00233.

Zalesky, A., Fornito, A., Harding, I. H., Cocchi, L., Yucel, M., Pantelis, C., et al. (2010). Whole-brain anatomical networks: Does the choice of nodes matter? *NeuroImage, 50*(3), 970–983.

Zhang, B., Xu, Y. H., Wei, S. G., Zhang, H. B., Fu, D. K., Feng, Z. F., et al. (2014). Association study identifying a new susceptibility gene (AUTS2) for schizophrenia. *International Journal of Molecular Sciences, 15*(11), 19406–19416.

Zhu, J., Zhuo, C., Xu, L., Liu, F., Qin, W., & Yu, C. (2017). Altered coupling between resting-state cerebral blood flow and functional connectivity in schizophrenia. *Schizophrenia Bulletin, 43*(6), 1363–1374.

Zielinski, B. A., Gennatas, E. D., Zhou, J., & Seeley, W. W. (2010). Network-level structural covariance in the developing brain. *Proceedings of the National Academy of Sciences of the United States of America, 107*(42), 18191–18196.

Zugman, A., Assuncao, I., Vieira, G., Gadelha, A., White, T. P., Oliveira, P. P., et al. (2015). Structural covariance in schizophrenia and first-episode psychosis: An approach based on graph analysis. *Journal of Psychiatric Research, 71*, 89–96.